Proceedings of the 35th European Safety and Reliability & the 33rd Society for Risk Analysis Europe Conference
Edited by Eirik Bjorheim Abrahamsen, Terje Aven, Frederic Bouder, Roger Flage, Marja Ylönen
 Published by Research Publishing, Singapore.
doi: 10.3850/978-981-94-3281-3_ESREL-SRA-E2025-P3221-cd

Prediction of Critical Heat Flux in Vertical Tubes by Physics-informed Neural Networks

Ibrahim Ahmed

Department of Energy, Politecnico di Milano, Milano, Italy. E-mail: ibrahim.ahmed@polimi.it

Irene Gatti

Department of Energy, Politecnico di Milano, Milano, Italy. E-mail: irene.gatti@mail.polimi.it

Enrico Zio

MINES Paris, PSL University, CRC, Sophia Antipolis, France. E-mail: enrico.zio@mines-paristech.fr
Department of Energy, Politecnico di Milano, Milano, Italy. E-mail: enrico.zio@polimi.it

The safety of thermohydraulic systems with two-phase flow is directly related to the Critical Heat Flux (CHF), which characterizes the transition from nucleate boiling to film boiling with a significant reduction of heat transfer efficiency. CHF prediction is crucial in nuclear power plants (NPPs), where thermohydraulic margins are critical for safe operation. Recent efforts to improve CHF prediction in vertical tubes have increasingly relied on data-driven approaches using Artificial Intelligence (AI) and Machine Learning (ML) techniques. Nevertheless, purely data-driven models often lack intrinsic physical information, limiting their broader acceptance for practical applications in safety-critical systems like NPPs. In this work, we explore the use of physics-informed neural networks (PINNs) for CHF prediction in vertical tubes. The Westinghouse (W-3) empirical correlation, an empirical CHF correlation developed by Westinghouse Electric Company for water-cooled reactors, is employed as the physical model integrated into the learning process of the PINN. Specifically, two different forms of physical loss function for PINN are formulated. The first form is based on simple differences (SD) between the predicted CHF from the model and the CHF calculated using W-3 correlation; the second form is based on partial derivatives (PD) of the W-3 correlation computed with respect to the input parameters. The developed PINN models are validated using experimental CHF data from the US Nuclear Regulatory commission (NRC), provided by the Working Party on Scientific Issues and Uncertainty Analysis of Reactor Systems (WPRS) Expert Group on Reactor Systems Multi-Physics (EGMUP) task force on AI/ML for Scientific Computing in Nuclear Engineering projects, promoted by the OECD/NEA. The results indicate that the predictive performance of the proposed PINN models exceeds those of the Look-Up Table (LUT) and purely data-driven deep neural networks, confirming the benefit of integrating physical knowledge into the learning process for enhancing accuracy and reliability of the prediction model.

Keywords: *Nuclear reactor safety, Thermohydraulic systems, Critical heat flux, Artificial intelligence, Physics-informed neural networks*.

1. Introduction

In the design of thermohydraulic systems involving two-phase flow, Critical Heat Flux (CHF) is a crucial concept to be considered. CHF is a parameter that marks the transition from nucleate to film boiling, leading to a significant reduction in heat transfer efficiency and to potential system failure (Bruder, Bloch, and Sattelmayer 2016). CHF plays a relevant role for the safety design of systems like nuclear reactors and steam generators (Chang and Baek 2003). For the operation of nuclear power plants (NPPs), CHF is a key parameter in relation to thermohydraulic margins and overall operational safety (Chang and Baek 2003). The departure from nucleate boiling ratio (DNBR) must be such to ensure safety, with the U.S. Nuclear Regulatory Commission (NRC) requiring a minimum DNBR of 1.3 (Todreas and Kazimi 2011). Despite extensive research, a

comprehensive physical description of CHF remains elusive due to the complexity of two-phase flow interactions (Bruder, Bloch, and Sattelmayer 2016).

CHF prediction models have evolved over the years from empirical correlations (Tong 1967; Katto 1992) and mechanistic models (Lee and Mudawwar 1988; Celata et al. 1999) to empirical methods such as CHF look-up tables (LUTs). The most widely used CHF LUT, developed by Groeneveld et al. in 2006, correlates CHF values across varying conditions (Doroshchuk, Levitan, and Lantzman 1975; Groeneveld 2019). Despite being effective, LUTs lack physical insights and contain data gaps. Recent advances in artificial intelligence (AI) and machine learning (ML) have introduced novel CHF prediction methods. In (Jiang and Zhao 2013), a hybrid model was developed by combining support vector regression (v-SVR) with radial basis function networks (RBFNs) to predict CHF, and the obtained results showed superior performance compared to standard SVR and empirical correlations approaches. In (He and Lee 2018), the work on v-SVR was extended to address sparsely distributed CHF data and demonstrated improved accuracy when focusing the training near critical inflection points. In (Khalid et al. 2024), an ensemble of deep sparse autoencoders (AEs) for feature extraction was developed and coupled with a deep neural network (DNN) as a meta-learner for CHF prediction. This method addressed the limitations of previous models by leveraging a large dataset that covered a wide range of operating conditions, thereby significantly enhancing prediction accuracy and reliability. In (Zhao et al. 2020), a hybrid framework that integrated ML with domain knowledge (physics-informed ML) was developed. This approach extended the applicability of the model and improved both generalization capabilities and predictive performance compared to traditional models. In (Mao and Jin 2024), ML models were combined with physical models to develop physics-informed ML (PIML) for CHF prediction, and the results showed that LUT-informed NN was the most stable and robust model.

While hybrid and ensemble models have improved prediction accuracy, optimizing their structure remains a challenge. It is essential to maintain a balance between complexity and overfitting, while ensuring meaningful performance improvements. To address this issue, (Ahmed, Gatti, and Zio 2025) proposed an optimized ensemble of neural network (NN) models that enhances prediction accuracy while mitigating model complexity for CHF predictions, thereby achieving a balance between ensemble complexity and performance improvements.

Although the above reviewed AI/ML-based approaches have contributed to improving CHF prediction accuracy, they are predominantly data-driven and, thus, lack physical insights. The studies in (Zhao et al. 2020; Mao and Jin 2024) mentioned the implementation of PIML, but involving primarily hybrid models that combine ML with empirical or LUT-based predictions. These models typically function as error-correction mechanisms, where ML models are trained on the errors in empirical or LUT-based predictions. The final CHF prediction is, then, obtained by adding the predicted error from the ML model with the CHF value from the empirical or LUT-based model. Such approaches lack explicit formulation of physical information within the learning process of AI/ML models.

To address this limitation, this work explores the use of physics-informed neural networks (PINNs) for CHF prediction in vertical tubes. Specifically, the Westinghouse (W-3) correlation (Tong 1967), an empirical CHF correlation developed by Westinghouse Electric Company for water-cooled reactors, is employed as the physical model integrated into the learning process of the PINNs. This correlation is simple, easy to implement, and suitable for both subcooled and saturated boiling conditions. Based on this empirical correlation, two distinct forms of physical loss function in PINNs are formulated: *1*) Simple Difference (SD) form, which is based on the difference between the CHF predicted by the model and the CHF calculated using the W-3 correlation; and *2*) Partial Derivative (PD) form, which is based on computing the PD of the W-3 correlation with respect to the input parameters, allowing the incorporation of CHF variations due to changes in these parameters. These two approaches enable the model to capture the local behavior of CHF with respect to each variable. By integrating these approaches into the PINN

framework, this work aims to enhance both prediction accuracy and generalization, bridging the gap between data-driven modeling and physically consistent CHF prediction. The proposed method is validated using experimental CHF data originally presented in (Groeneveld 2019) and made available by the Working Party on Scientific Issues and Uncertainty Analysis of Reactor Systems (WPRS) Expert Group on Reactor Systems Multi-Physics (EGMUP) task force on AI and ML for Scientific Computing in Nuclear Engineering projects, promoted by the OECD/NEA (LE CORRE et al. 2024). The obtained results show that the proposed method accurately predicts the CHF values under specific flow conditions, and significantly outperforms the traditional LUT-based approach.

The rest of the paper is organized as follows. Section 2 presents the problem formulation. The proposed PINN model for CHF prediction is described in Section 3 and the case study used to validate its performance is presented in Section 4. In Section 5, the results are presented and discussed. Finally, Section 6 presents the concluding remarks on the work performed.

2. Problem Formulation

In this paper, we consider a water-cooled nuclear reactor (a heat transfer system) at the design stage, for which accurate prediction of CHF is necessary for ensuring effective heat transfer. In this system, a set of laboratory measurements of P relevant physical variables, $\mathbf{x}_i$ are available under defined boundary conditions, at a generic observational point i:

$$\mathbf{x}_i = [x_{i,1}, \quad \cdots, \quad x_{i,j}, \quad \cdots, \quad x_{i,P}] \qquad (1)$$

These measured physical variables include both geometrical and hydraulic variables, such as hydraulic or equivalent tube diameter, heated length, pressure, mass flux and outlet quality. These variables affect the CHF phenomenon, q_i^{CHF}, directly or indirectly, at the same observational point i.

We assume the availability of the following:

(i) A physical model of the system describing the physical behavior of the CHF phenomenon, $q_i^{Corr}(\mathbf{x}_i)$;

(ii) A dataset $\boldsymbol{D} = [\mathbf{x}_i \quad q_i^{CHF}]_{i=1,\dots,N}$ containing the experimental measurements collected over a specific period of time, consisting of:

- the measurement matrix $\boldsymbol{X} \in \mathbb{R}^{N\times P}$, whose element $x_{i,j}$ is the measured physical quantity j at the observation point i, with $i = 1, \dots, N$ and $j = 1, \dots, P$;
- the corresponding CHF vector $\boldsymbol{q}^{CHF} \in \mathbb{R}^N$, which contains the CHF measurements q_i^{CHF} at each observation point i, with $i = 1, \dots, N$.

On the basis of the above assumptions, given a new vector of measurements $\mathbf{x}_{test}$ taken at the current observation, the objective of the present work is to develop a PINN model that integrates the physical model, $q_i^{Corr}(\mathbf{x}_i)$, into the learning process, which receives in input $\mathbf{x}_{test}$ and predicts in output the corresponding CHF value $\hat{q}_{test}^{CHF}$.

3. Proposed Method

The method developed for CHF prediction is sketched in Fig. 1. It consist of the development of the PINN model (Section 3.1) and the application of the developed model for CHF prediction (Section 3.2).

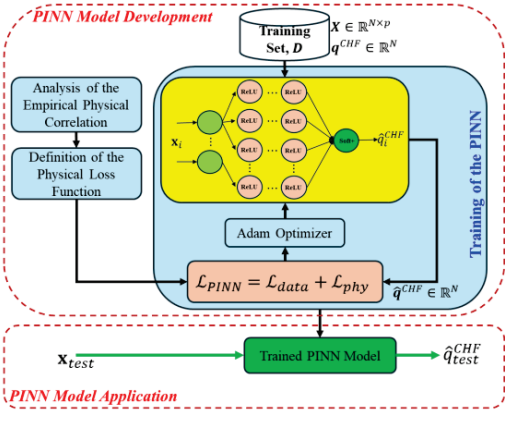

Fig. 1.Proposed PINN model for CHF prediction.

3.1. *Development of the PINN Model*

The development of the PINN model consists of the three key steps: *1*) analysis of the selected

empirical correlation to be integrated into the training process (Section 3.1.1); *2*) formulation of the PINN loss function (Section 3.1.2); and *3*) training of the PINN model (Section 3.1.3).

3.1.1. *Analysis of Empirical Correlation*

Due to its broad applicability in the nuclear industry and its ease of derivation, the Westinghouse correlation (W-3 correlation), developed by (Tong 1967) for predicting DNB under flow boiling conditions in nuclear reactor design has been selected for the implementation of the PINNs in this work.

The W-3 correlation highlights the significance of both the local DNB heat flux and its location. It was developed based on the primary parameters influencing flow patterns and CHF, namely local pressure, mass flux and thermodynamic quality. System pressure determines the saturation temperature and associated thermal properties, which, in turn, influence bubble size, buoyancy effects and the degree of subcooling required for bubble formation. By incorporating local enthalpy, the model accounts for subcooling effects on bubble dynamics. Through empirical fitting of available experimental data, (Tong 1967) formulated a correlation that integrates pressure (P), mass flux (G) and thermodynamic quality (X), along with local enthalpy (H_{in}) and tube diameter (D) as a geometric factor. Each function within the correlation was derived by plotting an independent parameter against measured CHF data while keeping all other variables constant (Tong and Tang 1997). The correlation for CHF is expressed as the product of multiple functional dependencies:

$$q''_{crit} = F(X,P) \cdot F(X,G) \cdot F(D) \cdot F(H_{in}) \qquad (2)$$

By explicitly deriving each function in Eq. (2), the W-3 correlation is obtained:

$$\begin{aligned} \frac{q''_{DNB}}{10^6} &= \left[(2.022 - 0.00043P) \right. \\ &\left. + (0.172 - 0.000098P)e^{(18.177-0.004P)X}\right] \\ &\cdot \left[(0.148 - 1.596X + 0.173X|X|)\frac{G}{10^6} \right. \\ &\left. + 1.037\right] \cdot [1.157 - 0.869X] \\ &\cdot [0.266 + 0.836e^{-3.151D}] \\ &\cdot [0.826 + 0.00079(H_{sat} - H_{in})] \end{aligned} \qquad (3)$$

where q''_{DNB} is expressed in Btu/hft^2. The parameter ranges for validity covered by the W-3 correlation and their respective units are summarized in Table 1.

Table 1. Validity ranges of the parameters for the W-3 Correlation.

Parameter	Range	Unit
P	$1000 - 2300$	psia
G	$1.0 \times 10^6 - 5.0 \times 10^6$	lb/hft^2
D	$0.2 - 0.7$	in
L	$10 - 144$	in
X	$-0.15 - +0.15$	-
H_{in}	≥ 400	Btu/hft^2

Although the W-3 correlation was originally derived for flow inside vertical tubes, it has demonstrated strong agreement with flow conditions outside fuel rod bundles when the hydraulic diameter is substituted for the actual tube diameter. When employing empirical correlations such as this to determine operating conditions and safety margins in nuclear reactors, highly conservative boundaries are typically implemented to ensure safe operation under all circumstances (Bruder, Bloch, and Sattelmayer 2016). However, reducing over-conservatism through innovative AI-driven approaches can provide significant economic benefits, including cost savings and increased productivity through the optimal utilization of available resources.

3.1.2. *Formulation of the PINN Loss Function*

In accordance with the International System of Units (SI), the validity ranges of the W-3 correlation parameters (Table 1) have been converted to the following values: 6.89–15.86 MPa for pressure, 1356–6781 kg/m^{2}s for mass flux, 0.005–0.018 m for diameter, 0.25–3.66 m for heated length, and ≥930 kJ/kg for inlet enthalpy. These conversions facilitate the direct application of the correlation to experimental datasets. The W-3 correlation, with adjusted coefficients to account for the transition to SI units, is expressed as:

$$
\begin{aligned}
&q^{Corr} \\
&= \left[(2.022 - 0.062P)\right. \\
&\left. + (0.172 - 0.014P)e^{(18.177-0.599P)X}\right] \\
&\cdot [(0.148 - 1.596X + 0.173X|X|)2.334G \\
&+ 3271] \cdot [1.157 - 0.869X] \\
&\cdot [0.266 + 0.836e^{-124D}] \\
&\cdot [0.826 + 0.00034(H_{sat} - H_{in})]
\end{aligned} \tag{4}
$$

Since the proposed PINN model aims to predict the actual CHF value, q_i^{CHF}, using five input parameters, $\mathbf{x}_i = [P_i,\ G_i,\ D_i,\ L_i,\ X_i]$, the PINN is designed such that the predicted CHF is:

$$\hat{q}_i^{CHF} = f_{\boldsymbol{\theta}}(\mathbf{x}_i) \tag{5}$$

where $\boldsymbol{\theta}$ is the vector of PINN weights, which are the trainable parameters optimized by minimizing the physically consistent loss function:

$$arg\min_{\boldsymbol{\theta}} \mathcal{L}_{PINN} \tag{6}$$

with

$$\mathcal{L}_{PINN} = (1 - \lambda)\mathcal{L}_{data} + \lambda\mathcal{L}_{phy} \tag{7}$$

where $\mathcal{L}_{data}$ is the data-driven loss function:

$$\mathcal{L}_{data} = \frac{1}{N}\sum_{i=1}^{N}(\hat{q}_i^{CHF} - q_i^{CHF})^2, \tag{8}$$

$\mathcal{L}_{phy}$ is the physical loss function, and λ is the hyperparameter that controls the relative importance assigned to $\mathcal{L}_{phy}$. The physical loss function is formulated using two distinct forms:

A. Simple difference (SD) form

This form is based on the simple differences (SD) between the predicted CHF from the model and the CHF calculated using the W-3 correlation (Eq. (4)). This form integrates into the learning process the physical relationships described by the correlation. The SD-based PINN loss function, $\mathcal{L}_{\text{phy}}$ is given by:

$$\mathcal{L}_{phy} = \frac{1}{N}\sum_{i=1}^{N}(\hat{q}_i^{CHF} - q_i^{Corr}) \tag{9}$$

B. Partial derivative (PD) form

This form is based on computing the partial derivatives (PD) of Eq. (4) with respect to the input parameters. The objective is to incorporate the variations in CHF due to changes in the input parameters, as described by the empirical correlation (Eq. (4)). This form captures the local behavior of CHF in relation to each variable. Specifically, the PD-based PINN loss function, $\mathcal{L}_{\text{phy}}$, is formulated as:

$$\mathcal{L}_{phy} = \frac{1}{N}\sum_{i=1}^{N}\left(\mathcal{L}_{D,i} + \mathcal{L}_{P,i} + \mathcal{L}_{G,i} + \mathcal{L}_{X,i}\right) \tag{10}$$

where

$$
\begin{cases}
\mathcal{L}_D = \left(\dfrac{\partial\hat{q}_i^{CHF}}{\partial D} - f_D'(D,P,G,X)\right)^2, \\
\mathcal{L}_P = \left(\dfrac{\partial\hat{q}_i^{CHF}}{\partial P} - f_P'(D,P,G,X)\right)^2, \\
\mathcal{L}_G = \left(\dfrac{\partial\hat{q}_i^{CHF}}{\partial G} - f_G'(D,P,G,X)\right)^2, \\
\mathcal{L}_X = \left(\dfrac{\partial\hat{q}_i^{CHF}}{\partial X} - f_X'(D,P,G,X)\right)^2,
\end{cases} \tag{11}
$$

Here $f_j'(\cdot)$ is the PD of the empirical CHF correlation, q^{Corr}, derived from Eq. (4) with respect to *j*-th input parameter; $\frac{\partial\hat{q}_i^{CHF}}{\partial x_{i,j}}$ is the PD of the predicted CHF from the PINN model with respect to the *j*-th input parameter, which can be efficiently computed using the Automatic Differentiation feature inherent in NNs.

3.1.3. *Training of the PINN Model*

Based on the PINN loss function forms formulated in Section 3.1.2, the PINN model is trained using the training dataset $\boldsymbol{D}$ by minimizing Eq. (6) with the Adam optimizer through the backpropagation algorithm.

3.2. *Application of the Trained PINN*

For a given test input $\mathbf{x}_{test}$ measured at the current observation, the trained PINN model (Fig. 1, bottom) receives in input $\mathbf{x}_{test}$ and provides in output the prediction of the CHF, $\hat{q}_{test}^{CHF}$.

4. Case Study

To validate the proposed CHF prediction model, the publicly available CHF experimental dataset published by the US Nuclear Regulatory Commission, originally from (Groeneveld 2019), is used. This dataset is a collection of 59 different experiments performed in vertical water-cooled uniformly heated tubes during the past decades and made available by the WPRS-EGMUP task force on AI and ML for Scientific Computing in Nuclear Engineering projects, promoted by the OECD/NEA (LE CORRE et al. 2024). The dataset contains 24579 observations of seven input parameters and one output variable (CHF). The input parameters include geometric (tube diameter, heated length), measured (pressure, mass flux, inlet temperature) and calculated (outlet quality, inlet subcooling) parameters, covering a wide range of system conditions. In this paper, only five input parameters (tube diameter, heated length, pressure, mass flux, outlet quality) are considered, following the recommendation of the benchmark organizer (LE CORRE et al. 2024). The data is partitioned into 80% for model development (training set) and 20% for model evaluation (test set).

To assess the performance of the developed PINN model on the test dataset $\boldsymbol{D}_{test} = [\mathbf{x}_i \quad q_i^{CHF}]_{i=1,\dots,N^t}$, the following metrics are employed (LE CORRE et al. 2024):

1) the root mean square percentage error (RMSPE), calculated as:

$$RMSPE = 100\sqrt{\frac{1}{N^t}\sum_{i=1}^{N^t}\left(\frac{\hat{q}_i^{CHF} - q_i^{CHF}}{q_i^{CHF}}\right)^2} \quad (9)$$

where N^t is the amount of data points in $\boldsymbol{D}_{test}$.

2) the mean absolute percentage error (MAPE), computed as:

$$MAPE = \frac{100}{N^t}\sum_{i=1}^{N^t}\left|\frac{\hat{q}_i^{CHF} - q_i^{CHF}}{q_i^{CHF}}\right| \quad (10)$$

3) Q^2-error, calculated as:

$$Q^2 = \frac{\sum_{i=1}^{N^t}(\hat{q}_i^{CHF} - q_i^{CHF})^2}{\sum_{i=1}^{N^t}(\hat{q}_i^{CHF} - \hat{\mu})^2} \quad (11)$$

where $\hat{\mu}$ is the mean of the measured CHF values, $\boldsymbol{q}^{CHF} \in \mathbb{R}^{N^t}$ in $\boldsymbol{D}_{test}$.

5. Results and Discussion

To determine the optimal PINN model, the weight of the physical loss, λ, is initially set to zero in Eq. (7), which results in a purely data-driven DNN model. In this case, various DNN architectures are explored by adjusting hyperparameters such as learning rate, number of layers, number of nodes (neurons) per layer and batch size using a grid search approach. Consequently, the optimal data-driven DNN model is obtained with five hidden layers made by 90, 70, 70, 60 and 60 neurons, respectively. The ReLU activation function is used in all layers except the output layer, where the softplus activation function is employed to ensure positive CHF predictions. Subsequently, by using the obtained DNN architecture, the PINN model $f_{\boldsymbol{\theta}}(\mathbf{x}_i)$ is developed and trained with the Adam optimizer using a learning rate of 0.0001, a batch size of 24, and a number of epochs of 900. To determine the optimal PINN model, the weight of the physical loss term, λ, in Eq. (7) is varied between 0 and 1 with step of 0.001 using a grid search approach and the optimal values is determined based on cross-validation prediction accuracy. Both proposed physical loss formulations (Eqs. (9) and (10)) are evaluated. The optimal values of λ are found to be 0.04 for the SD-based PINN and 0.001 for the PD-based PINN. Figure 2 compares the CHF prediction of the proposed PINN models with those of the LUT method on the test dataset, against measured experimental values. The results indicate that a higher proportion of CHF data points predicted by the PINN models fall within a ±10% error band than those predicted by the LUT. This demonstrates the effectiveness of the PINN models in capturing the input-output relationships underlying CHF, and the robust generalization capability.

The performance of the proposed PINN models have been verified by comparison to three state-of-the-art prediction methods based on LUT, Support Vector Regression (SVR) and DNN. The SVR model is trained and optimized using the same 80% training dataset used to develop the proposed models, whereas the DNN corresponds to the optimal purely data-driven DNN model obtained when λ is set to zero.

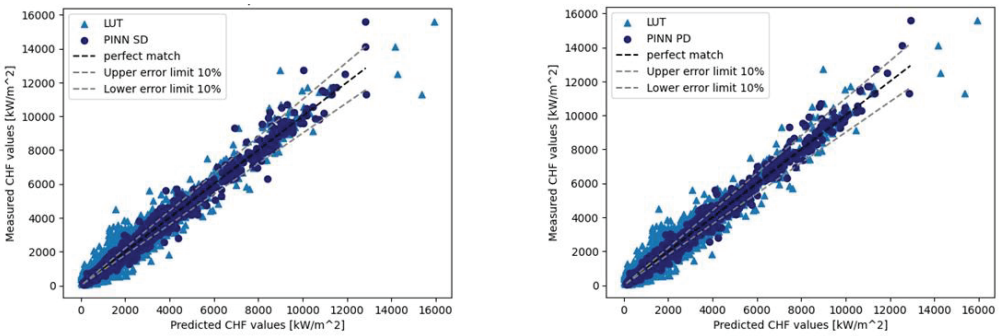

(a) (b)

Fig. 2. Predicted vs. measured CHF on test set for (a) SD-based PINN and (b) PD-based PINN.

Table 2. Comparison of the accuracy of CHF prediction models on the test set.

Model	Performance metrics			
	RMSPE	MAPE	$Q^2 - error$	Within ±20% error
LUT	43.05	22.31	0.0606	67.05%
SVR	20.75	12.28	0.0379	85.31%
DNN	16.61	10.13	0.0175	**88.20%**
SD-based PINN	17.00	**10.09**	0.0171	88.16%
PD-based PINN	**16.38**	10.29	**0.0168**	87.08%

Table 2 reports the values of the performance metrics obtained for each method. The results indicate that both the DNN and PINN models outperform the LUT and SVR approaches, with the PINN models demonstrating superior performance across nearly all metrics. Specifically, the PINN models (both SD-based PINN and PD-based PINN) achieve the lowest RMSPE and MAPE values, as well as the smallest Q^2-error, highlighting their strong predictive capability. This performance is attributed to the integration of physical information into the learning process, enhancing the accuracy and reliability of the model. It is important to note that although the SD-based PINN achieves the lowest MAPE value (10.09), the PD-based PINN exhibits superior overall performance, with the lowest RMSPE (16.38) and Q^2-error (0.0168). Furthermore, it significantly outperforms the SD-based PINN, which has an RMSPE of 17.00 and a Q^2-error of 0.0171. These results indicate that incorporating the partial derivatives of the empirical correlation (i.e., the rate of change of CHF with respect to variations in the input parameters) into the learning process of the AI/ML model is more effective than integrating the differences between the predictions of the empirical correlation and those of the AI/ML model.

6. Conclusions

This paper presents a new approach to CHF prediction in vertical tubes based on PINN models to enhance predictive accuracy and generalization capabilities. Specifically, information derived from the Westinghouse (W-3) correlation, an empirical CHF correlation developed by Westinghouse Electric Company for water-cooled reactors, is used as the physical model and integrated into the learning process of the PINN. Based on this correlation, two different forms of physical loss function for PINN are formulated. The first form is based on the simple differences (SD) between the CHF values predicted by the model and the CHF values calculated using the empirical correlation. This form integrates into the learning process the physical relationships described by the correlation. The second form is based on computing the partial derivatives (PD) of the correlation with respect to the input parameters. This form incorporates the variations in CHF

described by the empirical correlation due to changes in the input parameters, to capture the local behavior of CHF in relation to each variable. The proposed method is validated using experimental CHF data from the WPRS-EGMUP task force on AI/ML for Scientific Computing in Nuclear Engineering projects, promoted by the OECD/NEA. The obtained results show that the proposed PINN models achieve superior accuracy in CHF prediction, with lower errors across all metrics considered when compared to conventional methods such as the LUT approach and SVR. Furthermore, when compared the performance of the two formulated PINN models, it is found that incorporating into the learning process of the AI/ML model the PDs of the empirical correlation (i.e., the rate of change of CHF with respect to variations in the input parameters) is more effective than integrating the differences between the predictions of the empirical correlation and those of the AI/ML model.

Future research will focus on embedding multiple physical information within the NNs architecture, for the development of multi-physics-informed NNs which could further enhance the robustness and reliability of the models and increase the precision of the learning algorithm by incorporating multiple fundamental physical principles into the NN training process.

References

Ahmed, I., I. Gatti, and E. Zio. 2025. "Optimized Ensemble of Neural Networks for the Prediction of Critical Heat Flux." *Nuclear Engineering and Design* Under Revi.

Bruder, M., G. Bloch, and T. Sattelmayer. 2016. "Critical Heat Flux in Flow Boiling—Review of the Current Understanding and Experimental Approaches." *Heat Transfer Engineering* 38 (3): 347–360.

Celata, Gian Piero, Maurizio Cumo, Yoshiro Katto, and Antonio Mariani. 1999. "Prediction of the Critical Heat Flux in Water Subcooled Flow Boiling Using a New Mechanistic Approach." *International Journal of Heat and Mass Transfer* 42: 1457–66.

Chang, S., and W.-P. Baek. 2003. "Understanding, Predicting, and Enhancing Critical Heat Flux." In *The 10th Int. Topical Meeting on Nuclear Reactor Thermal Hydraulics (NURETH-10)*, October 5-9, 2003. Seoul, Korea.

CORRE, Jean-Marie LE LE, Gregory DELIPEI, Xu WU, and Xingang ZHAO. 2024. "Benchmark on Artificial Intelligence and Machine Learning for Scientific Computing in Nuclear Engineering. Phase 1: Critical Heat Flux Exercise Specifications."

Doroshchuk, V. E., I. L. Levitan, and F. P. Lantzman. 1975. "Investigation into Burnout in Uniformly Heated Tubes." *ASME Publication* 75.

Groeneveld, D. C. 2019. "Critical Heat Flux Data Used to Generate the 2006 Groeneveld Critical Heat Flux Lookup Tables."

He, Mingfu, and Youho Lee. 2018. "Application of Machine Learning for Prediction of Critical Heat Flux: Support Vector Machine for Data-Driven CHF Look-up Table Construction Based on Sparingly Distributed Training Data Points." *Nuclear Engineering and Design* 338: 189–198.

Jiang, B., and F. Zhao. 2013. "Combination of Support Vector Regression and Artificial Neural Networks for Prediction of Critical Heat Flux." *International Journal of Heat and Mass Transfer* 62: 481–494.

Katto, Yoshiro. 1992. "A Prediction Model of Subcooled Water Flow Boiling CHF for Pressure in the Range 0.1–20 MPa." *International Journal of Heat and Mass Transfer* 35: 1115–23.

Khalid, Rehan Zubair, Ibrahim Ahmed, Atta Ullah, Enrico Zio, and Asifullah Khan. 2024. "Enhancing Accuracy of Prediction of Critical Heat Flux in Circular Channels by Ensemble of Deep Sparse Autoencoders and Deep Neural Networks." *Nuclear Engineering and Design* 429: 113587.

Lee, C .H., and I. Mudawwar. 1988. "A Mechanistic Critical Heat Flux Model for Subcooled Flow Boiling Based on Local Bulk Flow Conditions." *International Journal of Multiphase Flow* 14 (6): 711–28.

Mao, Congshan, and Yue Jin. 2024. "Uncertainty Quantification Study of the Physics-Informed Machine Learning Models for Critical Heat Flux Prediction." *Progress in Nuclear Energy* 170: 105097.

Todreas, N.E., and M. Kazimi. 2011. *Nuclear Systems* Volume *I: Thermal Hydraulic Fundamentals*. Second Edi. CRC Press.

Tong, L. S. 1967. "Prediction of Departure from Nucleate Boiling for an Axially Non-Uniform Heat Flux Distribution." *Journal of Nuclear Energy* 21 (3): 241–248.

Tong, L. S., and Y. S. Tang. 1997. *Boiling Heat* Transfer *And Two-Phase Flow*. 1st ed. Routledge.

Zhao, Xingang, Koroush Shirvan, Robert K. Salko, and Fengdi Guo. 2020. "On the Prediction of Critical Heat Flux Using a Physics-Informed Machine Learning-Aided Framework." *Applied Thermal Engineering* 164: 114540.